Regular paper

Frequency reconfigurable stepped impedance dipole antenna for wireless applications

Manoj Mani, Remsha Moolat, Shameena V. Abdulrahiman, Anila P. Viswanathan, Vasudevan Kesavath, Mohanan Pezholil

PII: S1434-8411(19)31792-3
DOI: https://doi.org/10.1016/j.aeue.2019.153029
Reference: AEUE 153029

To appear in: *International Journal of Electronics and Communications*

Received Date: 17 July 2019
Revised Date: 6 November 2019
Accepted Date: 9 December 2019

Please cite this article as: M. Mani, R. Moolat, S.V. Abdulrahiman, A.P. Viswanathan, V. Kesavath, M. Pezholil, Frequency reconfigurable stepped impedance dipole antenna for wireless applications, *International Journal of Electronics and Communications* (2019), doi: https://doi.org/10.1016/j.aeue.2019.153029

Frequency reconfigurable stepped impedance dipole antenna for wireless applications

Manoj Mani[1], Remsha Moolat[1], Shameena V. Abdulrahiman[1] , Anila P Viswanathan[1,2],

Vasudevan Kesavath[1] and Mohanan Pezholil[1]

[1]Centre for Research in Electromagnetics and Antenna, Department of Electronics, Cochin University of Science and Technology, Kochi, Kerala, India.

[2]M A College of Engineering, Kothamangalam.

E mail:manojmelpadam@gmail.com, remsha398@gmail.com, shameenava@gmail.com, anilapv@gmail.com, vasudevankdr@gmail.com, drmohan@gmail.com.

Corresponding author- Mohanan Pezholil, Email: **drmohan@gmail.com**

Abstract—A stepped impedance (SI) based frequency tunable dipole antenna for WLAN (2.4-2.48 GHz) / Bluetooth (2.4 – 2.48 GHz) / LTE (2-2.7 GHz)/ wireless power transfer/ UMTS (2.1 GHz)/ WiMAX (2.5-2.7 GHz) applications has been investigated in this paper. The proposed antenna has an overall dimension of 0.408 λ_0 × 0.245 λ_0 × 0.013 λ_0, where λ_0 represents the free-space wavelength at the frequency 2.45 GHz. By embedding varactor diodes on the SI dipole antenna arms and varying the bias voltage, the effective electrical length of the antenna can be changed, leading to an electrically tunable antenna without changing the length of the antenna. The simulation and experiments are well matched and offer a 2:1 VSWR (S11 < -10dB) bandwidth of 780 MHz. Experimental results show that by trimming the varactor diode, the operating frequency of the antenna can be electrically tuned from 1.98 to 2.76 GHz.

Keywords— Dipole antenna, Frequency reconfigurable antenna, Stepped impedance, Varactor diode, WLAN.

1 | INTRODUCTION

There has been an increasing demand for compact reconfigurable antennas in modern wireless communication systems, because of its superior features such as reconfigurable capability, multipurpose operation, low cost with an added advantage of miniaturization. Generally, reconfigurability can be applied to the resonant frequency, the direction of the main beam, beamwidth, and polarization [1-5]. By changing the effective length of the radiator, the antenna resonance frequency can be reconfigured. This concept of reconfigurability can be achieved by using either the microelectromechanical switches (MEMS) or solid-state devices, usually positive-intrinsic-negative (PIN) diodes and varactor diodes [6-11].

A stepped impedance-based reconfigurable filter is presented in [12], which uses four PIN diodes as switching elements. Stepped impedance dipole antennas are reported in [13, 14]. The pattern reconfigurable parasitic antenna using a pin diode is demonstrated in [15]. The integration of varactor diode along with the printed monopole antenna results in the frequency reconfigurability [16]. Variable chip capacitors are also used to control the antenna resonant frequency [17]. In the previously published articles, the technique presented to achieve frequency reconfigurability is more complicated [18], [19], and difficult to achieve in practical scenarios. The air gap between the substrate and ground plane is utilized to lower the effective permittivity of the antenna. For the proper tuning of the antenna resonant frequency, the thickness of the air gap should be trimmed. These require an additional mechanical system to adjust the air gap between substrate and ground plane for frequency reconfigurability, which is a very difficult task in practice. This mechanical adjusting system will also affect the antenna performance, such as bandwidth, gain, and size of the antenna.

In this paper, a novel compact and efficient frequency reconfigurable stepped impedance dipole

antenna for various wireless applications has been presented. A compact frequency reconfigurable antenna is achieved by increasing the electrical length of the antenna radiating element using varactor diodes on each arm of the dipole antenna. The proposed dipole antenna has advantages such as low cost, compact size, easy to fabricate, simple integration, omnidirectional radiation pattern, and optimum efficiency and gain.

All the numerical simulations and optimizations were performed using a time-domain solver in CST microwave studio. The reflection coefficient for the fabricated prototype as a function of source frequency was measured using an Agilent PNA E8362B. All the far-field radiation characteristics are measured in the anechoic chamber.

2 | DESIGN AND GEOMETRY OF THE ANTENNA

The geometry of the proposed stepped impedance (SI) dipole antenna is shown in **Fig. 1**. The antenna is realized on a substrate of $\varepsilon_r = 4.4$, $\tan\delta = 0.02$ and height $h = 0.013\ \lambda_0$, with copper trace thickness (t) of 35 μm. The antenna is made from two types of metallic strips of width W_p and W_t.

The proposed dipole antenna has an overall dimension of $0.408\ \lambda_0 \times 0.245\ \lambda_0 \times 0.013\ \lambda_0$. Fig. 1b shows the photograph of the fabricated antenna. The prototype of the proposed SI dipole antenna with optimized dimensions is fabricated using a standard photolithography process. Each arm of the SI dipole antenna is formed by two stepped impedances $Z_1 = 100\ \Omega$ and $Z_2 = 15\ \Omega$. The Z_1 and Z_2 are calculated from the widths W_t and W_p, respectively. The electrical length of the dipole arm is formed by $L_a = 0.081\lambda_0$ and $L_t = L_b + L_c + L_d + L_e + L_f = 0.0947\lambda_0$. The L_t is folded as in Fig. 1a to reduce the size of the antenna. In stepped impedance resonators (SIR) the fundamental frequency and higher harmonics are calculated from the values of impedance ratio (K) and length ratio (α). The impedance ratio of the SIR is given by $K = Z_2/Z_1$, and the length ratio is given by $\alpha = L_a/(L_t + L_a)$. The optimized values of K and α for the

proposed dipole antenna at 2.45 GHz are 0.15 and 0.43. The optimum parameters of the SI dipole antenna are tabulated in Table 1. From exhaustive studies in stepped impedance resonator (SIR) geometries, it is found that maximum separation between fundamental and first resonance is obtained by properly choosing K values of the SIR [20]. Similarly, the optimum value for length ratio (α) is found from the universal curve given in the above paper. By selecting k and α, the antenna design parameters Z_1, Z_2, L_t, and L_a can be easily derived for any desired frequency on a substrate.

The spacing between the switching metallic strips and position of the varactor diodes are optimized using simulation. Through the simulation, it is observed that for 0.06 mm, the spacing between the metallic strips with varactor diode gives good impedance matching at desired frequency bands. As shown in figure 1a, a chip inductor of 36 nH is linking the switching metallic strip and, bias lines isolate RF signal and DC source. A variable DC power supply of 30 V is used to control the operation of the varactor diode switch.

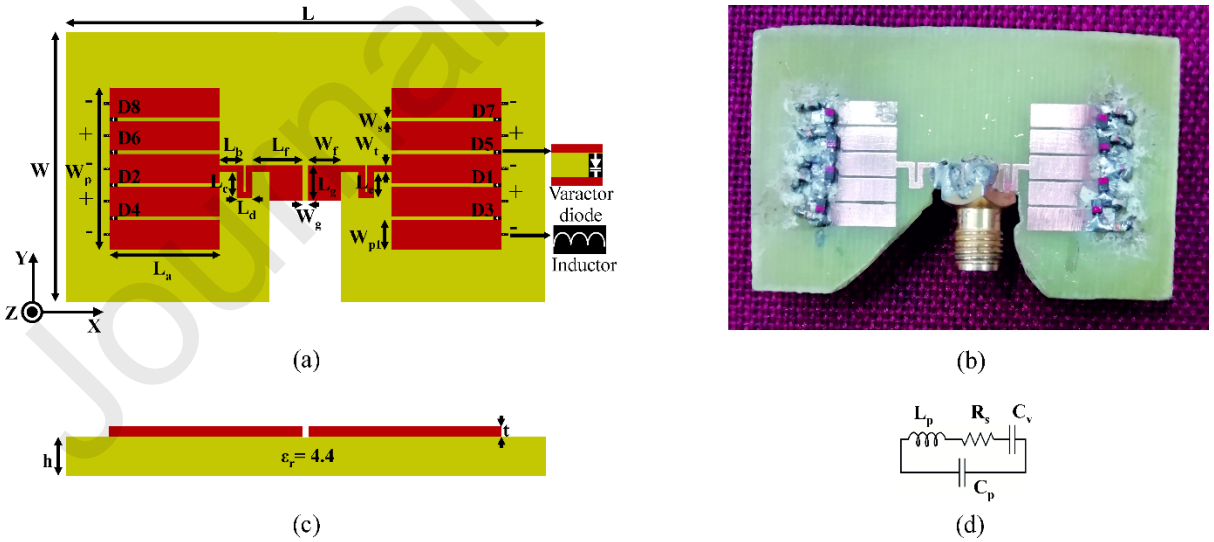

FIG. 1. Geometry of the proposed antenna. (a) Top view (b) Fabricated prototype of the antenna operating at 2.45 GHz, εr= 4.4, tan δ = 0.02 and height h = 0.013 λ_0. (c) side view (d) Varactor diode equivalent circuit.

Table 1.

Dimensions of the SI reconfigurable dipole antenna in **Fig. 1**.

Parameter	Dimensions	Parameter	Dimensions
L	0.408 λ_0	W	0.245 λ_0
L_a	0.081 λ_0	W_g	0.00408 λ_0
L_b	0.0163 λ_0	W_p	0.12 λ_0
L_c, L_e	0.0179 λ_0	W_{p1}	0.022 λ_0
L_d	0.00163 λ_0	W_s	0.00245 λ_0
L_f	0.0408 λ_0	W_t	0.0049 λ_0
L_g, W_f	0.0245 λ_0	h	0.013 λ_0

3 | RESULTS AND DISCUSSION

The simulated and measured reflection coefficients of the frequency reconfigurable dipole antenna without activating varactor diodes are shown in **Fig. 2**. The antenna is well-matched and operating at 2.45 GHz. The measured -10 dB bandwidth of the antenna is 420 MHz from 2.24 - 2.66 GHz. Varactor diodes are placed at gap W_s between the metallic strips of the dipole arm to switch the frequency for various applications. Silicon variable capacitance diode is used to vary the capacitance between two consecutive metallic strips.

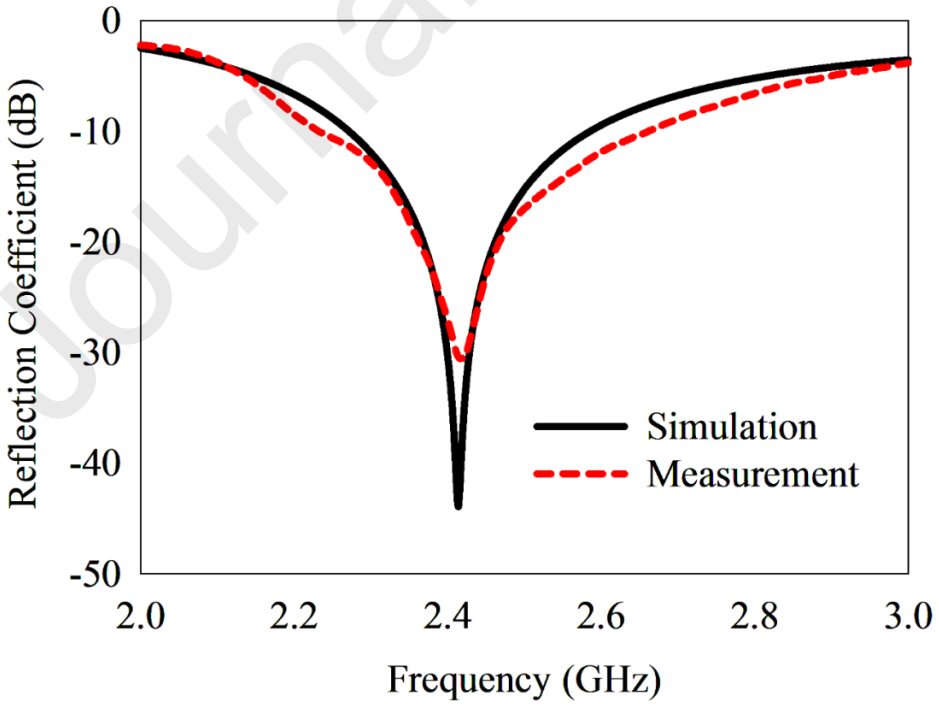

FIG. 2. Reflection coefficient of the frequency reconfigurable antenna without varactor diodes.

By tuning the varactor diode capacitance (C_v) as a function of reverse voltage (Vr), the resonant frequency of the antenna can be tuned, and the antenna can be made frequency reconfigurable. To investigate the frequency reconfigurability of the SI dipole antenna, a varactor diode is selected to cover the required capacitance. The selected silicon variable capacitance diode BB640 E6327 manufactured by Infineon is used in this study, and its equivalent circuit is shown in **Fig. 1**d. The capacitance of the intrinsic device C_v can be tuned from 77 to 3.7 pF when the reverse bias voltage is varied from 0 - 25 V, respectively. The capacitance values for the corresponding reverse voltage levels are tabulated in **Table 2**. The manufacturer gives the values of parasitic elements in the equivalent circuit of the varactor diode as L_p= 1.8 nH, C_p= 12 pF, and R_s= 1.15Ω.

Table 2

Capacitance values corresponds to the reverse bias voltage of varactor diode.

Reverse bias voltage (V)	Capacitance (pF)
0	77
5	55
10	13
15	7
20	4.2
25	3.7

The simulated and measured reflection coefficients of the proposed dipole antenna for different configurations of the varactor diodes are shown in **Fig.3**. Simulation studies are carried out by designing varactor diodes as RLC lumped element model. The values for R, L, and C are chosen from the datasheet of varactor diode. The capacitance values of the varactor diode vary with applied reverse bias voltage. To study the switching characteristics of the dipole antenna, four pairs of varactor diodes are used.

In the first case of switching, diodes D1 and D2 are enabled, the remaining diodes and inductors are disabled. The simulated and measured reflection coefficient of the dipole antenna, using a single varactor diode on each arm of the dipole are depicted in **Fig. 3**a and b, respectively. Using diode D1 and D2, the proposed antenna can operate in six different frequencies, as tabulated in **Table 3**. It is noted that in this case, the bandwidth of the antenna is 520 MHz, and these bands are well suited for the application bands LTE 2300 (2.3-2.4 GHz), LTE 2500 (2.5-2.69 GHz), WLAN (2.4 GHz), and Bluetooth (2.4 GHz).

In the second case, the diodes D3 and D4 are also enabled, hence the frequency reconfigurability is achieved with the aid of four varactor diodes D1, D2, D3, and D4. With two varactor diodes in each arm, the characteristics are different and are shown in **Fig. 3**c, and d. In this case, the switching frequency range starts from 2.04 to 2.42 GHz. Fig. 3c and d gives simulation and measured results and both are in reasonable agreement and suitable for wireless power transfer application at 2.4 GHz. The slight change in the simulation and measurement reflection coefficients of the antenna are shown in Fig. 3a-f are due to the presence of long dc wires in the measurement process that were not considered in the simulation. At the application band frequency (2.4 GHz), the obtained percentage bandwidth is 17.42 and is tabulated in **Table 3**.

Similarly, the diodes D5 and D6 are also enabled in the third case; in this case, diodes D1 to D6 are activated. The measured and simulated reflection coefficients of the antenna with three pairs of varactor diodes are shown in **Fig.3**e and f, respectively.

In the fourth case, all four pairs of varactor diodes from D1-D8 are activated. The Fig. 3g and h depicts the simulated and measured reflection coefficients of the antenna with all varactor diodes enabled. Switching resonance frequencies and operating bands for this case

is also tabulated in Table 3. In this case, the antenna has sufficient bandwidth to cover the entire UMTS (1.92 - 2.1 GHz) band.

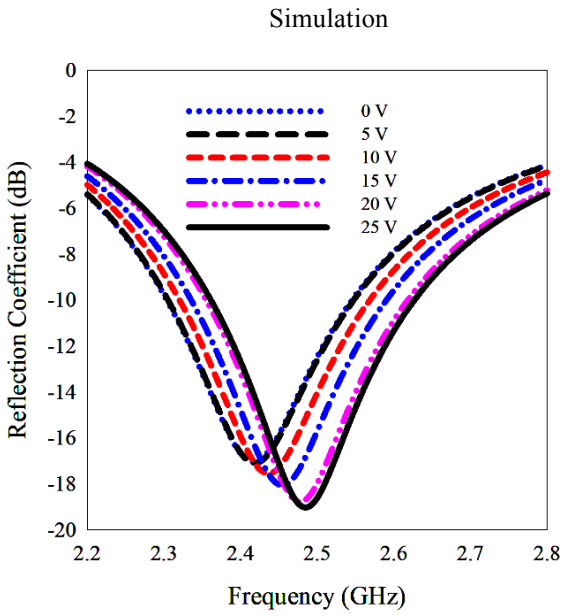

(a)

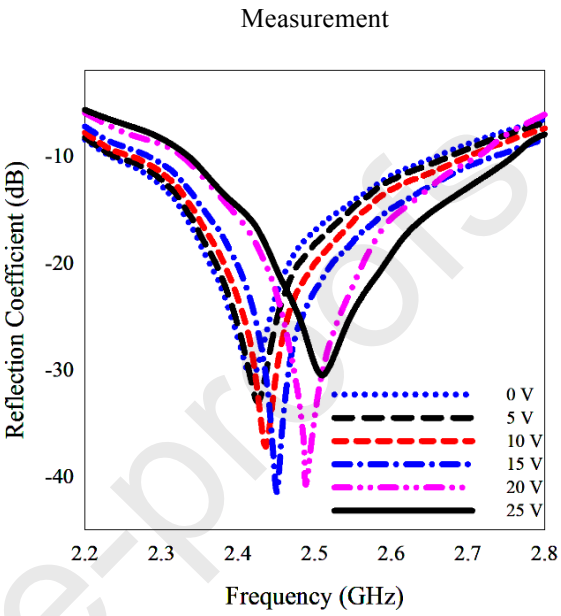

(b)

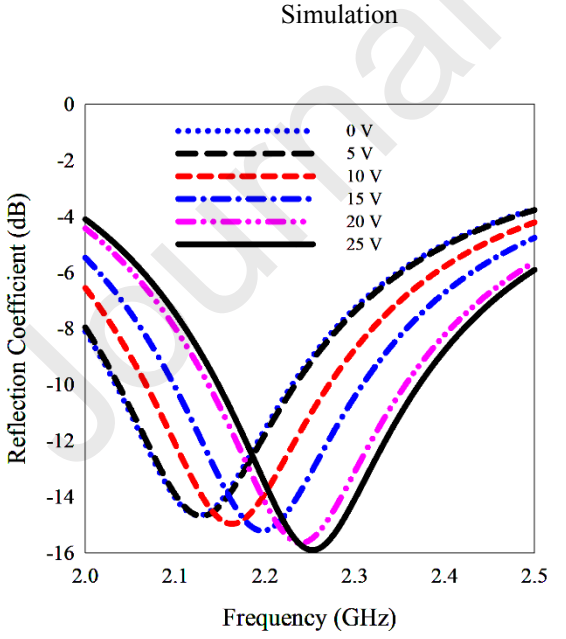

(c)

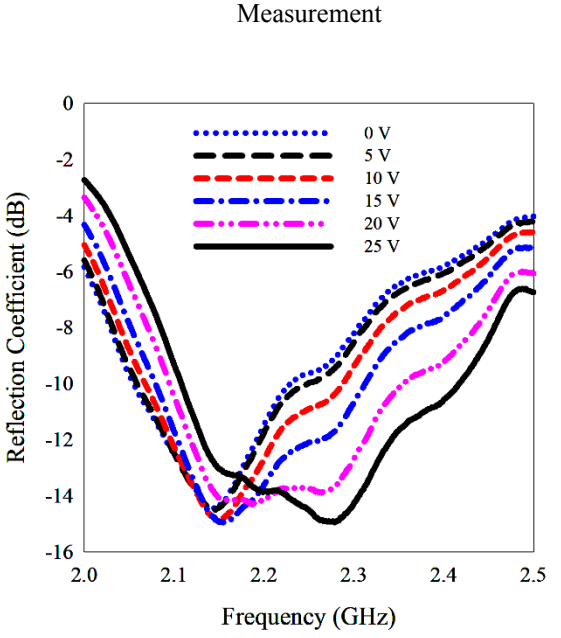

(d)

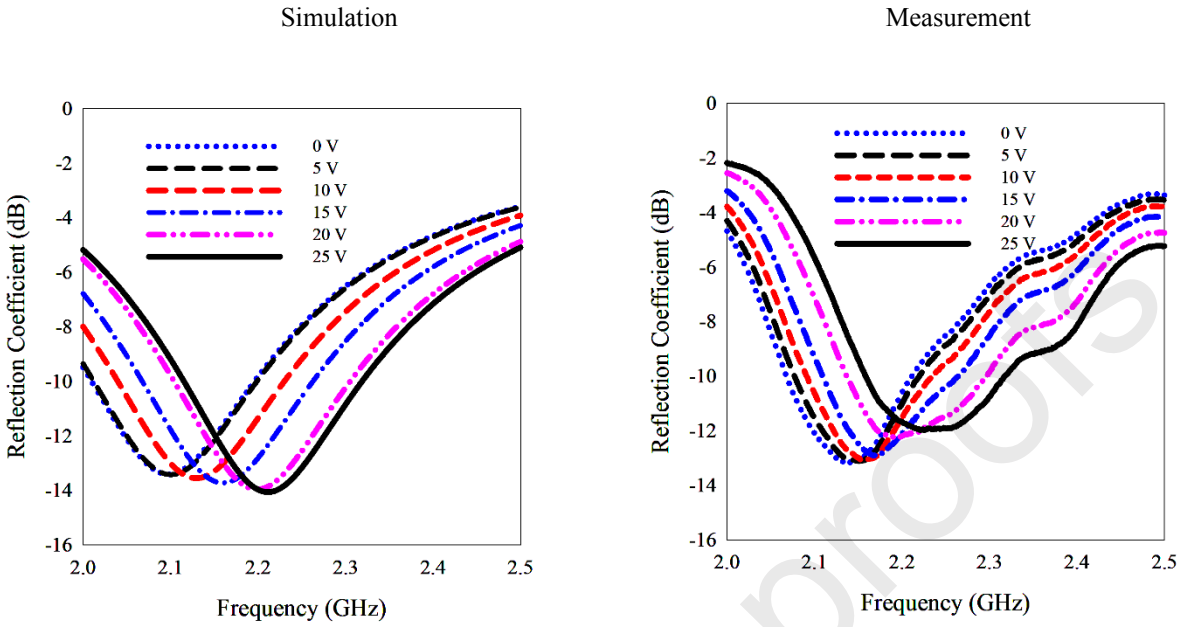

(e) (f)

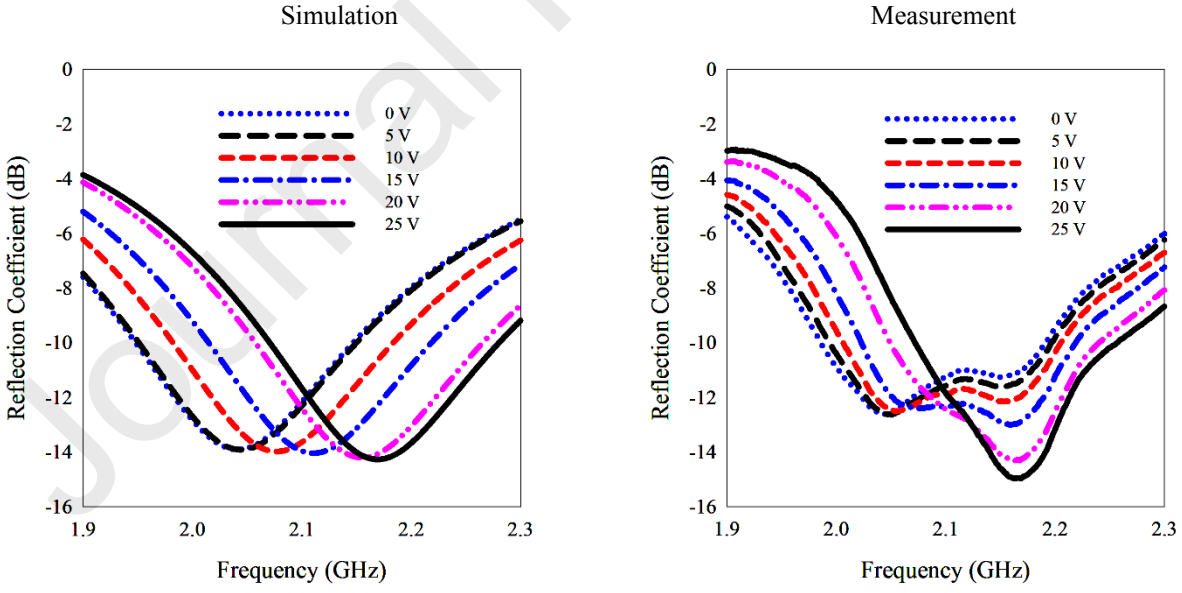

(g) (h)

FIG. 3. Frequency switching, (a, b) using single varactor diode on each arm of the SI dipole, (c,d) pair of varactor diodes on each arm of the SI dipole, (e,f) switching using 3 varactor diodes on each arm of the SI dipole, (g,h) 4 varactor diodes are used in each arm of the SI dipole.

Table 3

Simulated and measured resonant frequency switching of the SI dipole antenna.

Diodes enabled	Reverse voltage applied (V)	Switching resonant frequency fo (GHz), Reflection coefficient (dB)		Operation Band (GHz), Percentage of bandwidth (%)	
		Simulation	Measurement	Simulation	Measurement
D1, D2	0	2.41, -43	2.41, -30.5	2.27-2.57, 12.44	2.24-2.66, 17.42
	5	2.418, -17	2.42, -33	2.30-2.54, 9.9	2.23-2.65, 17.36
	10	2.43, -18	2.43, -37	2.31-2.56, 10.2	2.27-2.68, 16.87
	15	2.45, -18	2.45, -41	2.33-2.59, 10.61	2.29-2.70, 16.73
	20	2.495, -28	2.48, -40.5	2.35-2.61, 10.42	2.33-2.71, 15.32
	25	2.485, -20	2.51, -30.5	2.36-2.62, 10.46	2.34-2.76, 16.73
D1, D2, D3, D4	0	2.12, -14.6	2.14, -14	2.02-2.2, 8.4	2.04-2.22, 8.41
	5	2.13, -14.6	2.145, -14	2.05-2.21, 7.5	2.05-2.25, 9.32
	10	2.16, -15	2.15, -14	2.08-2.25, 7.87	2.06-2.28, 10.23
	15	2.19, -15	2.155, -15	2.11-2.29, 8.2	2.08-2.31, 10.67
	20	2.24, -15	2.18, -14	2.15-2.34, 8.48	2.09-2.35, 11.92
	25	2.25, -15	2.27, -15	2.16-2.36, 8.88	2.1-2.42, 14.09
D1, D2, D3, D4, D5, D6	0	2.09, -13.4	2.137, -13	2-2.19, 9	2.05-2.20, 7.01
	5	2.1, -13.4	2.1513, -13	2.01-2.19, 8.57	2.07-2.21, 6.5
	10	2.13, -13.4	2.1575, -13	2.04-2.23, 8.9	2.09-2.23, 6.4
	15	2.16, -13.7	2.1713, -13	2.06-2.26, 9.2	2.10-2.26, 7.36
	20	2.19, -14	2.195, -12	2.1-2.3, 9.1	2.13-2.29, 7.28
	25	2.21, -14	2.2213, -12	2.11-2.31, 9	2.16-2.31, 6.75
D1, D2, D3, D4, D5, D6, D7, D8	0	2.04, -14	2.04, -12.5	1.94-2.14, 9.8	1.98-2.18, 9.78
	5	2.05, -14	2.05, -12.5	1.95-2.15, 9.7	1.99-2.19, 9.75
	10	2.07,-14	2.053, -12.5	1.98-2.18, 9.6	2-2.22, 10.71
	15	2.11, -14	2.15, -13	2.01-2.21, 9.4	2.02-2.22, 9.3
	20	2.15, -14	2.163, -14	2.05-2.26, 9.7	2.04-2.24, 9.24
	25	2.169, -14	2.1645, -15	2.07-2.28, 9.6	2.07-2.26, 8.77

The simulated and measured normalized gain patterns of the antenna at 2.45 GHz without activating varactor diodes are shown in Fig. 4a. Fig 4b-e presents the simulated and measured normalized gain patterns when the antenna operates in four switching cases tabulated in Table. 3. The simulated and measured radiation patterns of the SI dipole antenna at 2.5 GHz with diodes D1 and D2 are active is shown in Fig. 4b. Similarly, the effect of activation of the diodes D1-D4 on the radiation pattern at 2.3 GHz is shown in Fig. 4c. In the third case of switching, the antenna radiation patterns at 2.2 GHz is depicted in Fig. 4d. The simulated and measured radiation patterns for the frequency of 2.1 GHz with all varactor diodes are activated (D1-D8) are plotted in Fig. 4e. All the measured and simulated radiation patterns are omnidirectional. The small differences in measured and simulated results are due to the spurious radiation from wires used for biasing the varactor diodes.

.

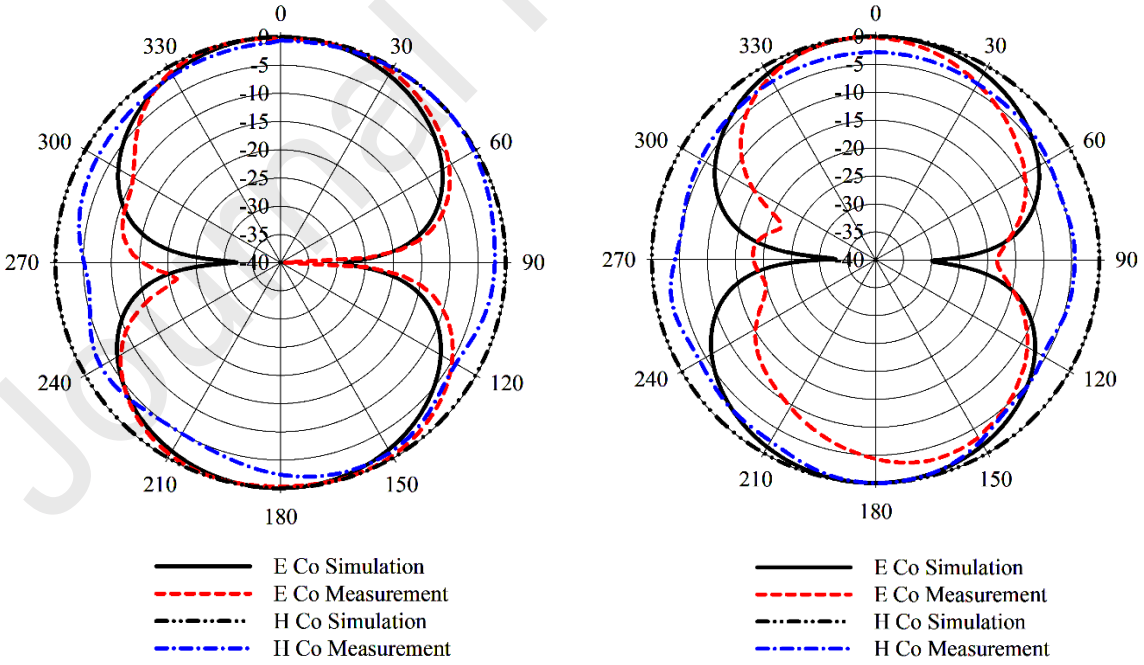

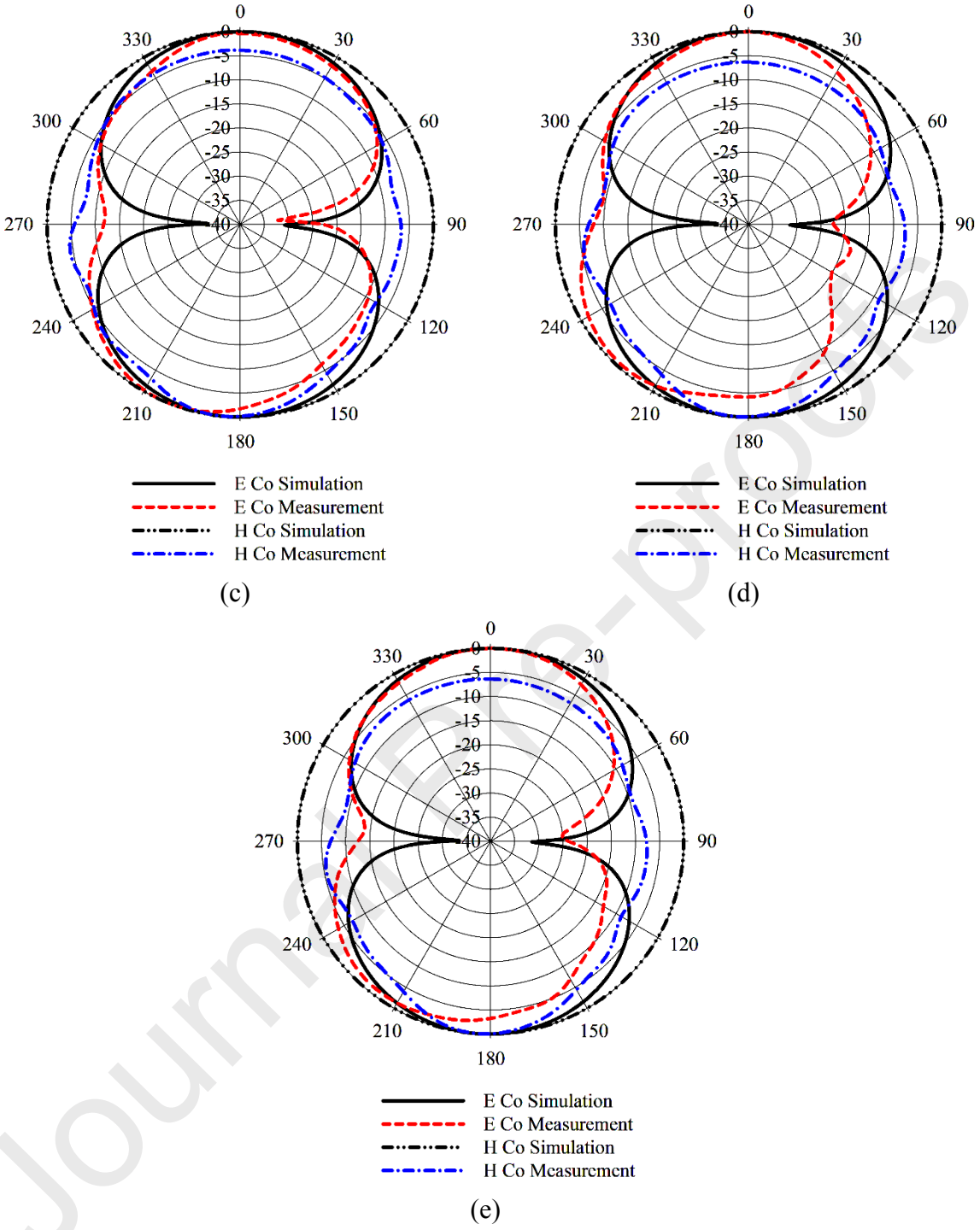

Fig. 4. Normalized omni directional radiation patterns (a) without any varactor diodes (b) single varactor diode on each arm (D1, D2) (c) two varactor diodes on each arm (D1, D2, D3, D4) (d) three varactor diodes on each arm (D1, D2, D3, D4, D5, D6) (e) four varactor diodes on each arm (D1, D2, D3, D4, D5,D6, D7, D8).

The measured cross-polar levels of the antenna for various switching cases are tabulated in Table 4. From Table 4, it is evident that for all the cases, the normalized cross-polarization is below -20 dB in both E- and H- planes. This shows that the embedded varactor diodes have a small impact on the cross-polar radiation patterns of the antenna.

Table 4
Measured cross-polarization levels of the SI dipole antenna.

Diodes Enabled	Without varactor diodes	D1,D2	D1,D2, D3,D4	D1,D2,D3, D4,D5,D6	D1,D2,D3,D4, D5,D6,D7,D8
E cross (dB)	-31	-32	-27	-22	-25
H cross (dB)	-33	-36	-26	-36	-33

The peak realized gain and efficiency of the reconfigurable antenna is also measured in the anechoic chamber, and the results are plotted in **Fig. 5**. The gain comparison method is used to measure the gain, and the wheeler cap method is used to measure the radiation efficiency of the SI dipole antenna.

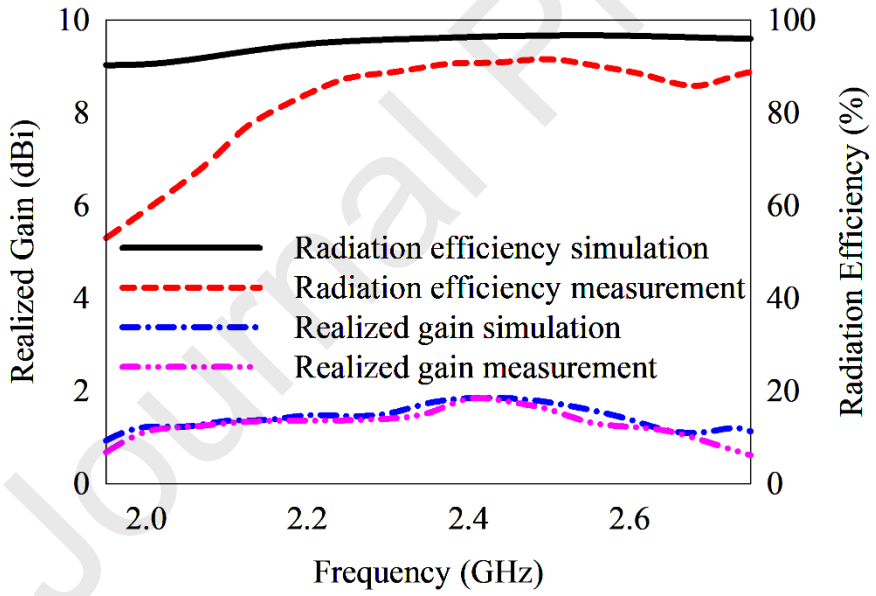

Fig. 5. Realized gain and efficiency of the antenna

From Fig. 5, it is clear that the simulated and measured gain plots are in good agreement. The peak realized a gain of the antenna is 1.8 dBi at 2.45 GHz. From **Fig. 5**, it is estimated that the measured efficiency is lower than that of the simulated efficiency. The measured radiation efficiency of the antenna varies from 51% to 92%. The decrease in the antenna efficiency at

lower frequency is due to the higher loss in the internal resistance of the varactor diode [21-24].

4 | CONCLUSION

The optimized stepped impedance frequency reconfigurable dipole antenna was simulated, fabricated, and measured. Four pairs of varactor diodes are used to tune the antenna frequency from 1.98-2.76 GHz for various wireless applications such as WLAN, Bluetooth, LTE 2300, LTE 2400, and UMTS. The measured radiation patterns of the antenna at different switching frequencies are omnidirectional and are in good agreement with simulation. Measured peak realized gain and efficiency of the proposed dipole antenna are found to be 1.8 dBi and 92%, respectively.

5 | ACKNOWLEDGEMENT

The authors acknowledge the University Grants Commission of Government of India and the Department of Science and Technology (DST) for financial assistance.

REFERENCES

[1] Anantha B, Merugu L, Somasekhar Rao P V.D. A novel single feed frequency and polarization reconfigurable microstrip patch antenna. AEU - Int J Electron Commun 2017;72:8–16. doi:10.1016/j.aeue.2016.11.012.

[2] Khairnar V V., Kadam B V., Ramesha CK, Gudino LJ. A reconfigurable parasitic antenna with continuous beam scanning capability in H-plane. AEU - Int J Electron Commun 2018;88:78–86. doi:10.1016/j.aeue.2018.02.014.

[3] Chen XF, Zhao YJ. Dual-band polarization and frequency reconfigurable antenna using double layer metasurface. AEU - Int J Electron Commun 2018;95:82–7. doi:10.1016/j.aeue.2018.08.001.

[4 Silveira E dos S, Fabiani BM, de Pina MVP, do Nascimento DC. Polarization reconfigurable microstrip phased array. AEU - Int J Electron Commun 2018;97:220–8. doi:10.1016/j.aeue.2018.10.023.

[5] Yang LS, Yang L, Zhu YA, Yoshitomi K, Kanaya H. Polarization reconfigurable slot antenna for 5.8 GHz wireless applications. AEU - Int J Electron Commun 2019;101:27–

32. doi:10.1016/j.aeue.2019.01.022.

[6] Mansour A, Tayel AF, Khames A, Azab M, Rabia SI, Shehata N. Towards software defined antenna for cognitive radio networks through appropriate selection of RF-switch using reconfigurable antenna array. AEU - Int J Electron Commun 2019;102:25–34. doi:10.1016/j.aeue.2019.01.033.

[7] Borakhade DK, Pokle SB. Pentagon slot resonator frequency reconfigurable antenna for wideband reconfiguration. AEU - Int J Electron Commun 2015;69:1562–8. doi:10.1016/j.aeue.2015.06.012.

[8] Kishore N, Prakash A, Tripathi VS. A reconfigurable ultra wide band antenna with defected ground structure for ITS application. AEU - Int J Electron Commun 2017;72:210–5. doi:10.1016/j.aeue.2016.12.009.

[9] Ali T, Muzammil Khaleeq M, Biradar RC. A multiband reconfigurable slot antenna for wireless applications. AEU – Int J Electron Commun 2018;84:273–80. doi:10.1016/j.aeue.2017.11.033.

[10] Yadav R, Patel PN. EBG-inspired reconfigurable patch antenna for frequency diversity application. AEU - Int J Electron Commun 2017;76:52–9. doi:10.1016/j.aeue.2017.03.022.

[11] Varamini G, Keshtkar A, Naser-Moghadasi M. Compact and miniaturized microstrip antenna based on fractal and metamaterial loads with reconfigurable qualification. AEU - Int J Electron Commun 2018;83:213–21. doi:10.1016/j.aeue.2017.08.057.

[12] Quddious A, Abbasi MAB, Saghir A, Arain S, Antoniades MA, Polycarpou A, et al. Dynamically reconfigurable SIR filter using rectenna and active booster. IEEE Trans Microw Theory Tech 2019;67:1504–15. doi:10.1109/TMTT.2019.2891524.

[13] Manoj M, Remsha M, Vinisha C V, Mohanan P. Stepped Impedance Resonator Based Uniplanar Dipole Antenna with Harmonic Suppression. 2018 IEEE Antennas Propag Soc Int Symp Usn Natl Radio Sci Meet APSURSI 2018 - Proc 2018:1747–8. doi:10.1109/APUSNCURSINRSM.2018.8608316.

[14] Remsha M, Manoj M, Shameena V A, P. Mohanan. SIR based Broadband Dipole Antenna for LTE/ WiMAX/ WLAN Applications. 2019 URSI Asia-Pacific Radio Sci Conf (AP-RASC)-proc 2019:1-3. doi: 10.23919/URSIAP-RASC.2019.8738220.

[15] Tang MC, Duan Y, Wu Z, Chen X, Li M, Ziolkowski RW. Pattern reconfigurable, vertically polarized, low-profile, compact, near-field resonant parasitic antenna. IEEE Trans Antennas Propag 2019;67:1467–75. doi:10.1109/TAP.2018.2883635.

[16] Mirzaei H, Eleftheriades G V. A Compact Frequency-Reconfigurable Metamaterial-Inspired Antenna. IEEE Antennas Wirel Propag Lett 2011;10:1154–7. doi:10.1109/LAWP.2011.2172180.

[17] Yang SS, Kishk AA, Lee K. Frequency Reconfigurable U-Slot Microstrip Patch Antenna. Antenna 2008;7:127–9. doi:10.1109/LAWP.2008.921330.

[18] Zohur A, Mopidevi H, Rodrigo D, Unlu M, Jofre L, Cetiner BA. RF MEMS reconfigurable two-band antenna. IEEE Antennas Wirel Propag Lett 2013;12:72–5. doi:10.1109/LAWP.2013.2238882.

[19] Zhu HL, Liu XH, Cheung SW, Yuk TI. Frequency-Reconfigurable Antenna Using Metasurface. IEEE Trans Antennas Propag 2013;62:80–5. doi:10.1109/tap.2013.2288112.

[20] Mani M, Moolat R, Vasudevan K, Mohanan P. Harmonic suppressed compact stepped impedance uniplanar dipole antenna for WLAN applications. Prog Electromagn Res Lett 2018;79. doi:10.2528/PIERL18080603.

[21] Nguyen-Trong N, Hall L, Fumeaux C. A frequency- and pattern-reconfigurable center-shorted microstrip antenna. IEEE Antennas Wirel Propag Lett 2016;15:1955–8. doi:10.1109/LAWP.2016.2544943.

[22] Qin PY, Guo YJ, Cai Y, Dutkiewicz E, Liang CH. A reconfigurable antenna with frequency and polarization agility. IEEE Antennas Wirel Propag Lett 2011;10:1373–6. doi:10.1109/LAWP.2011.2178226.

[23] Nguyen-Trong N, Kaufmann T, Fumeaux C, Hall L. Analysis and Design of a Reconfigurable Antenna Based on Half-Mode Substrate-Integrated Cavity. IEEE Trans Antennas Propag 2015;63:3345–53. doi:10.1109/TAP.2015.2434389.

[24] Ge L, Luk KM. Frequency-reconfigurable low-profile circular monopolar patch antenna. IEEE Trans Antennas Propag 2014;62:3443–9. doi:10.1109/TAP.2014.2318077.

Frequency reconfigurable stepped impedance dipole antenna for wireless applications

List of Figures

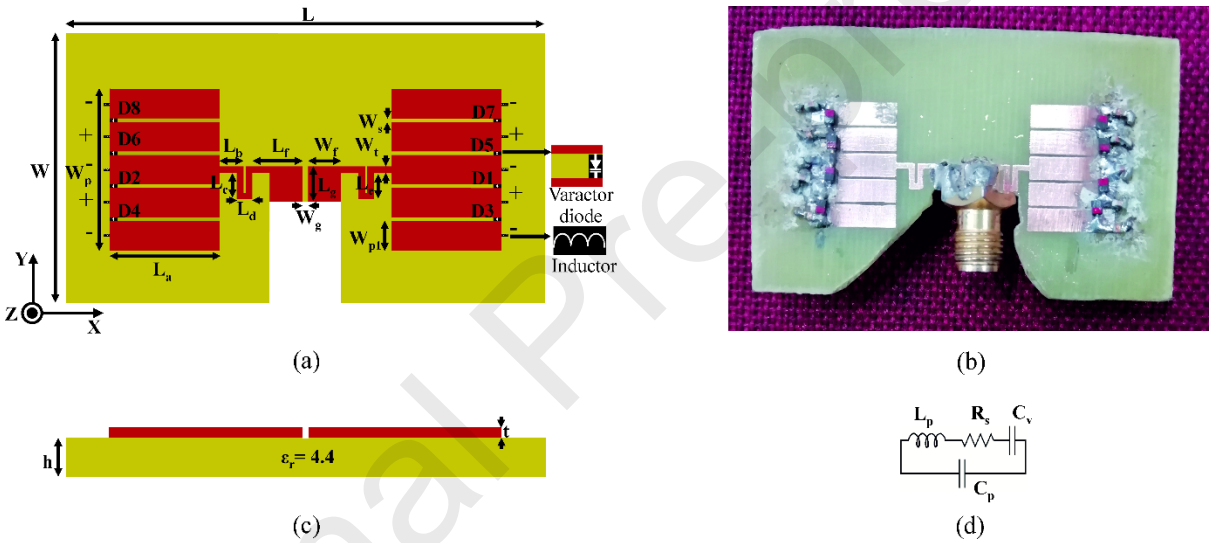

FIG. 1. Geometry of the proposed antenna. (a) Top view (b) Fabricated prototype of the antenna operating at 2.45 GHz, εr= 4.4, tan δ = 0.02 and height h = 0.013 λ0. (c) side view (d) Varactor diode equivalent circuit.

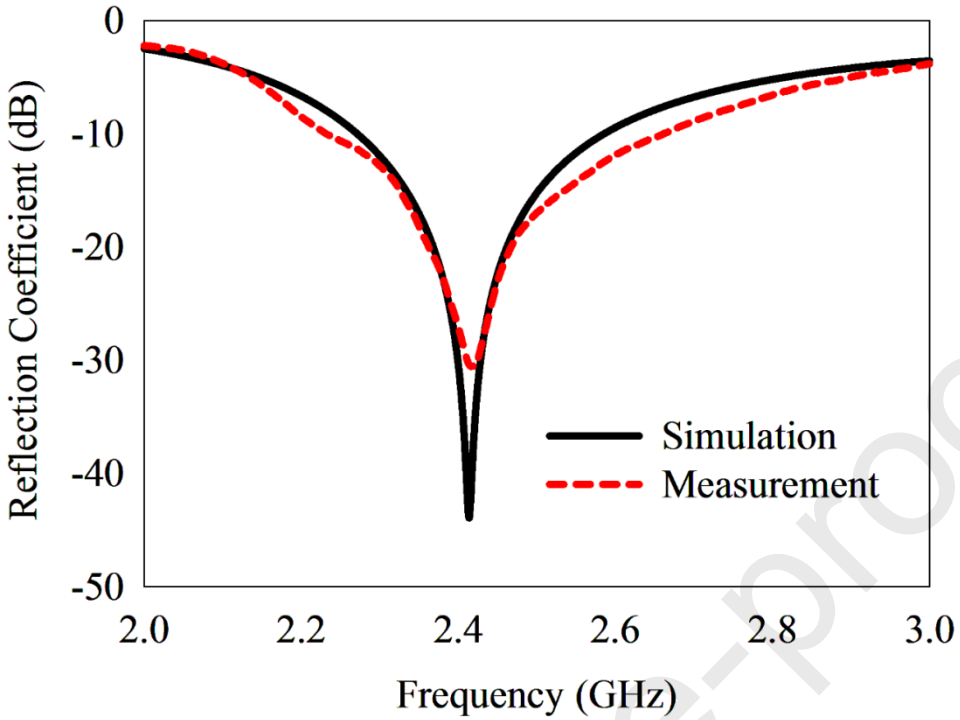

FIG. 2. Reflection coefficient of the frequency reconfigurable antenna without varactor diodes antenna

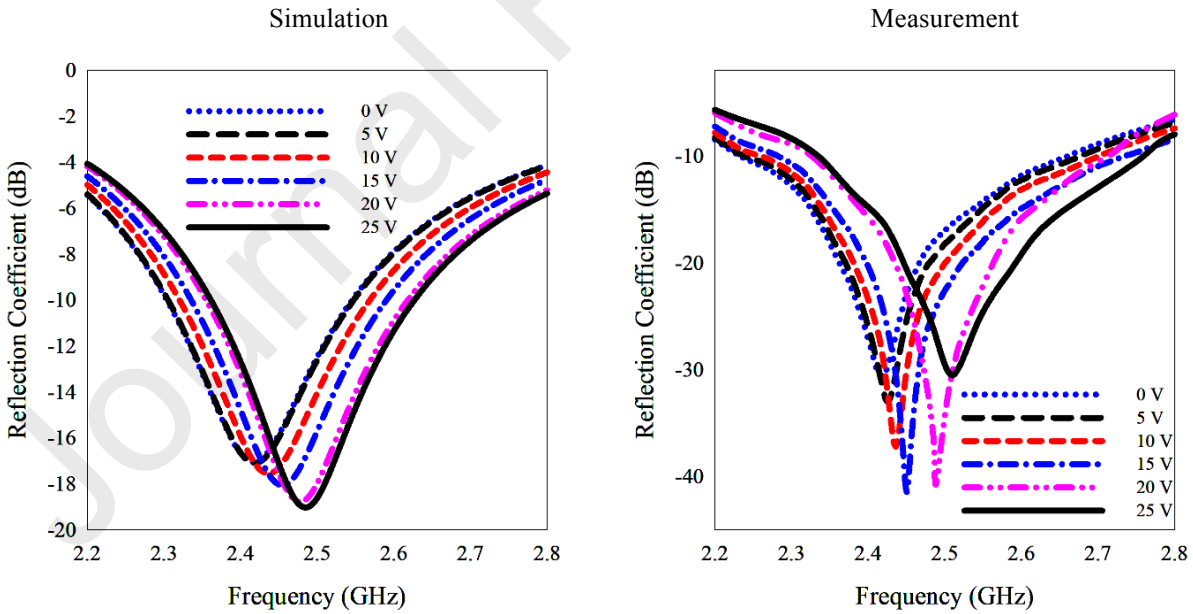

(b) (b)

Simulation

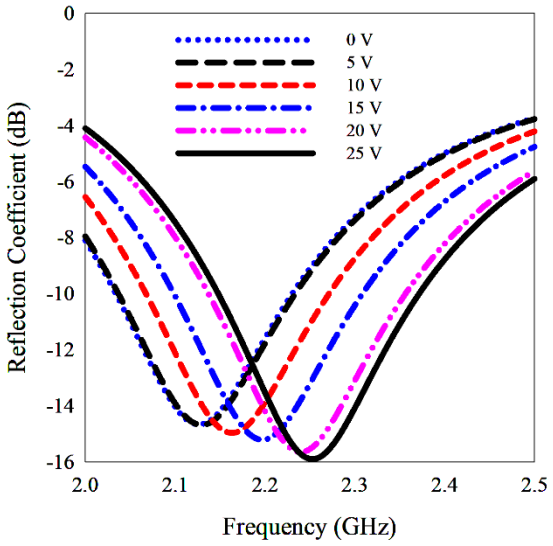

(c)

Measurement

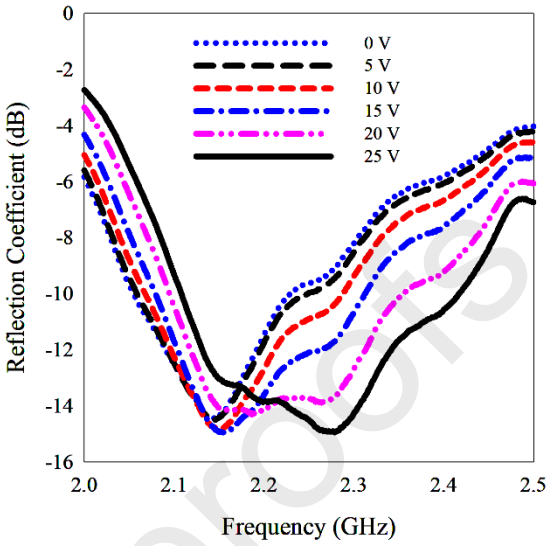

(d)

Simulation

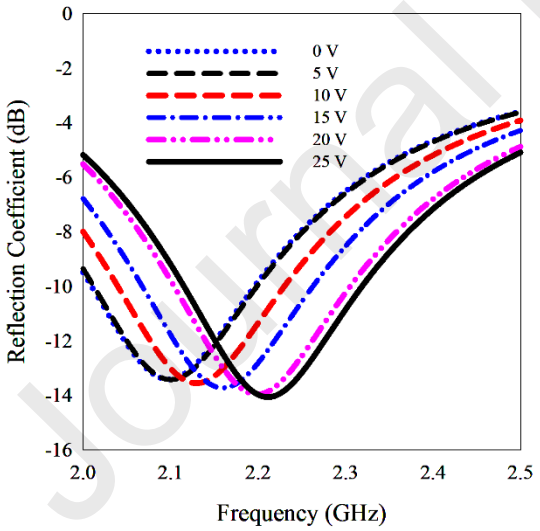

(e)

Measurement

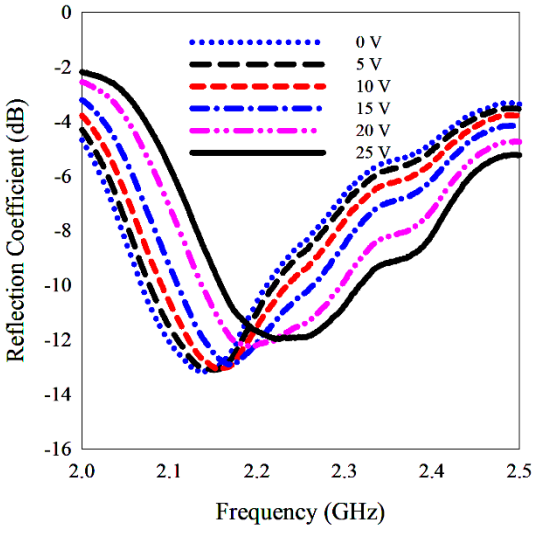

(f)

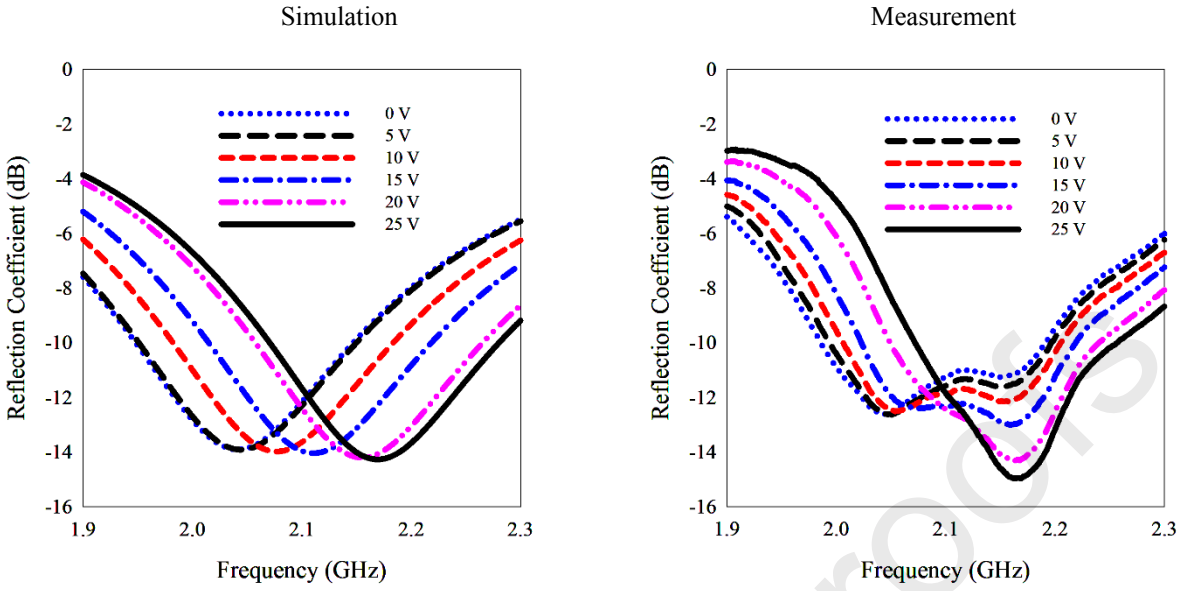

(g) (h)

FIG. 3. Frequency switching, (a, b) using single varactor diode on each arm of the SI dipole, (c,d) pair of varactor diodes on each arm of the SI dipole, (e,f) switching using 3 varactor diodes on each arm of the SI dipole, (g,h) 4 varactor diodes are used in each arm of the SI dipole.

.

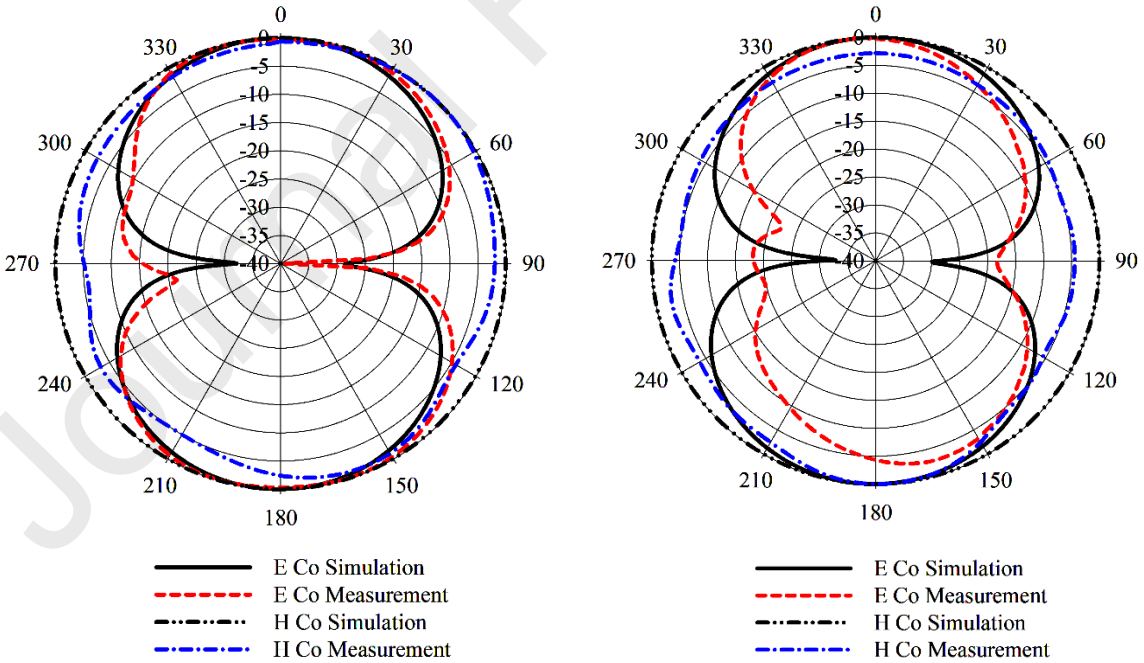

(a) (b)

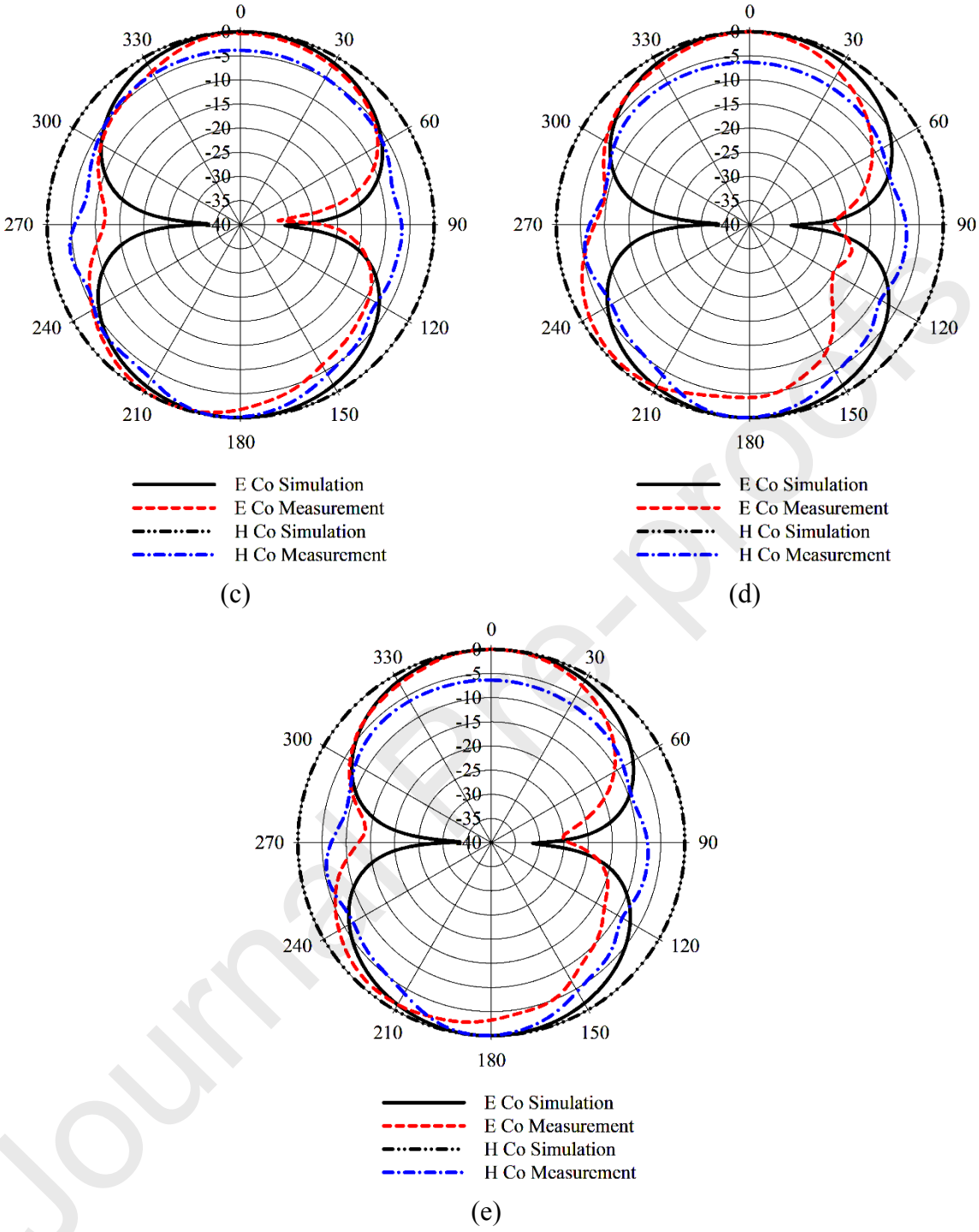

Fig. 4. Normalized omni directional radiation patterns (a) without any varactor diodes (b) single varactor diode on each arm (D1, D2) (c) two varactor diodes on each arm (D1, D2, D3, D4) (d) three varactor diodes on each arm (D1, D2, D3, D4, D5, D6) (e) four varactor diodes on each arm (D1, D2, D3, D4, D5,D6, D7, D8).

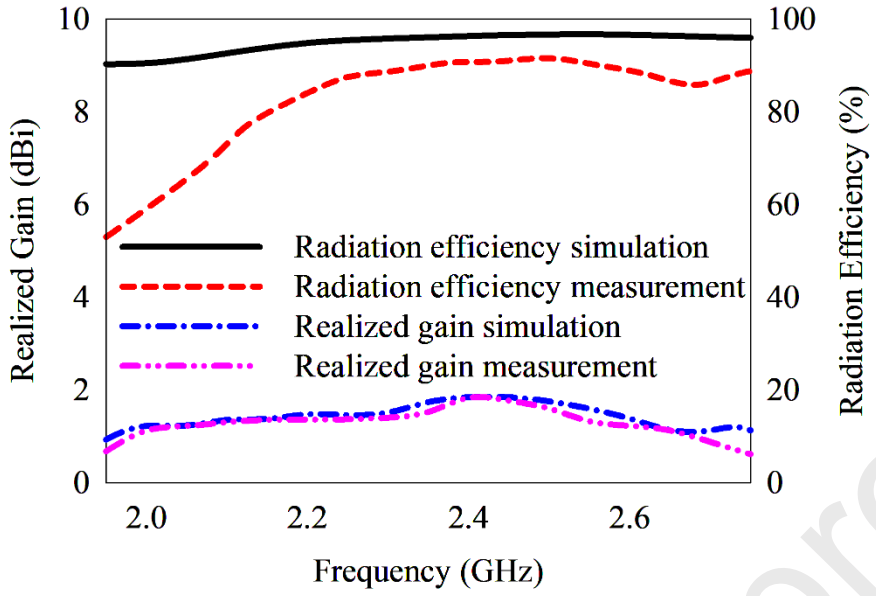

Fig. 5. Realized gain and efficiency of the antenna

Frequency reconfigurable stepped impedance dipole antenna for wireless applications

List of Tables

Table 1.

Dimensions of the SI reconfigurable dipole antenna in **Fig. 1**.

Parameter	Dimensions	Parameter	Dimensions
L	0.408 λ_0	W	0.245 λ_0
L_a	0.081 λ_0	W_g	0.00408 λ_0
L_b	0.0163 λ_0	W_p	0.12 λ_0
L_c, L_e	0.0179 λ_0	W_{p1}	0.022 λ_0
L_d	0.00163 λ_0	W_s	0.00245 λ_0
L_f	0.0408 λ_0	W_t	0.0049 λ_0
L_g, W_f	0.0245 λ_0	h	0.013 λ_0

Table 2

Capacitance values corresponds to the reverse bias voltage of varactor diode.

Reverse bias voltage (V)	Capacitance (pF)
0	77
5	55
10	13
15	7
20	4.2
25	3.7

Table 3

Simulated and measured resonant frequency switching of the SI dipole antenna.

Diodes enabled	Reverse voltage applied (V)	Switching resonant frequency fo (GHz), Reflection coefficient (dB)		Operation Band (GHz), Percentage of bandwidth (%)	
		Simulation	Measurement	Simulation	Measurement
D1, D2	0	2.41, -43	2.41, -30.5	2.27-2.57, 12.44	2.24-2.66, 17.42
	5	2.418, -17	2.42, -33	2.30-2.54, 9.9	2.23-2.65, 17.36
	10	2.43, -18	2.43, -37	2.31-2.56, 10.2	2.27-2.68, 16.87
	15	2.45, -18	2.45, -41	2.33-2.59, 10.61	2.29-2.70, 16.73
	20	2.495, -28	2.48, -40.5	2.35-2.61, 10.42	2.33-2.71, 15.32
	25	2.485, -20	2.51, -30.5	2.36-2.62, 10.46	2.34-2.76, 16.73
D1, D2, D3, D4	0	2.12, -14.6	2.14, -14	2.02-2.2, 8.4	2.04-2.22, 8.41
	5	2.13, -14.6	2.145, -14	2.05-2.21, 7.5	2.05-2.25, 9.32
	10	2.16, -15	2.15, -14	2.08-2.25, 7.87	2.06-2.28, 10.23
	15	2.19, -15	2.155, -15	2.11-2.29, 8.2	2.08-2.31, 10.67
	20	2.24, -15	2.18, -14	2.15-2.34, 8.48	2.09-2.35, 11.92
	25	2.25, -15	2.27, -15	2.16-2.36, 8.88	2.1-2.42, 14.09
D1, D2, D3, D4, D5, D6	0	2.09, -13.4	2.137, -13	2-2.19, 9	2.05-2.20, 7.01
	5	2.1, -13.4	2.1513, -13	2.01-2.19, 8.57	2.07-2.21, 6.5
	10	2.13, -13.4	2.1575, -13	2.04-2.23, 8.9	2.09-2.23, 6.4
	15	2.16, -13.7	2.1713, -13	2.06-2.26, 9.2	2.10-2.26, 7.36
	20	2.19, -14	2.195, -12	2.1-2.3, 9.1	2.13-2.29, 7.28
	25	2.21, -14	2.2213, -12	2.11-2.31, 9	2.16-2.31, 6.75
D1, D2, D3, D4, D5, D6, D7, D8	0	2.04, -14	2.04, -12.5	1.94-2.14, 9.8	1.98-2.18, 9.78
	5	2.05, -14	2.05, -12.5	1.95-2.15, 9.7	1.99-2.19, 9.75
	10	2.07,-14	2.053, -12.5	1.98-2.18, 9.6	2-2.22, 10.71
	15	2.11, -14	2.15, -13	2.01-2.21, 9.4	2.02-2.22, 9.3
	20	2.15, -14	2.163, -14	2.05-2.26, 9.7	2.04-2.24, 9.24
	25	2.169, -14	2.1645, -15	2.07-2.28, 9.6	2.07-2.26, 8.77

Table 4

Measured cross-polarization levels of the SI dipole antenna.

Diodes Enabled	Without varactor diodes	D1,D2	D1,D2, D3,D4	D1,D2,D3, D4,D5,D6	D1,D2,D3,D4, D5,D6,D7,D8
E cross (dB)	-31	-32	-27	-22	-25
H cross (dB)	-33	-36	-26	-36	-33

Conflict of interests

The authors declare that they have no known competing financial interests or personal relationships that could have appeared to influence the work reported in this paper.